Microphase Reorientation in Block Copolymer Melts As Detected via FT Rheology and 2D SAXS

M. Langela,[†] U. Wiesner,[§] H. W. Spiess,[‡] and M. Wilhelm*[,‡]

polyMaterials AG, Innovapark 20, 87600 Kaufbeuren, Germany; Max-Planck-Institut für Polymerforschung, Ackermannweg 10, 55128 Mainz, Germany; and Cornell University, Ithaca, New York

Received September 4, 2001

ABSTRACT: The alignment kinetics of the orientation/reorientation behavior of the microphase of a lamellarPS-*b*-PI diblock copolymer under large-amplitude oscillatory shear conditions is studied. By online monitoring the degree of the mechanical nonlinearity during the orientation process—as determined via the higher harmonics in Fourier transform (FT) rheology—and investigation of the orientational distribution by 2-dimensional small-angle X-ray scattering, we followed the kinetics of the microphase alignment for two different experimental shear conditions. Improved parallel alignment after increasing the shear frequency as well as spatially heterogeneous alignment via bimodal: parallel and perpendicular alignment of the lamellae is detected by both methods. Thus, FT rheology offers a new and simple way for online monitoring complex reorientation kinetics.

Introduction

Many industrial processes operate with high strain rates and/or high shear rates that often cause nonlinear mechanical effects like structural orientation.[1,2] As an example, microphase-separated diblock copolymers tend to orient their microstructure during rheological processes.[3−6] Diblock copolymers consist of two chemically distinct repeat units, which are separated in two blocks. The two blocks can undergo microphase separation depending on the interaction parameter χ of the monomers and the degree of polymerization N.[7−10] The symmetry of the microstructure varies with the volume fraction of the two polymer phases.[11−17] The present study concerns a block copolymer with a volume fraction of 50% for each block, which results generally in a lamellar morphology.

Microstructural orientation of block copolymers can cause, for example, birefringence or anisotropies in tensile strength. Therefore, it is advantageous to develop and apply tools that can determine the time evolution of alignment kinetics during a macroscopic orientation process. In the literature in-situ rheooptical methods are described[18,19] to guide electron microscopy (TEM) and X-ray scattering (SAXS) studies of the structure development during flow-induced alignment in a lamellar block copolymer melt. The progress of shear-induced alignment was recorded in real time using flow birefringence, and samples were taken at selective points of the alignment development for ex-situ characterization by TEM and SAXS. Two other approaches are in-situ small-angle X-ray scattering rheology[20,22] and in-situ small-angle neutron scattering rheology,[23] which both can follow the alignment kinetics without external analysis of the sheared sample. The experimental setups of all three methods are a combination of a rheometer for the application of shear flow and an online device for in-situ measurement of the alignment kinetics.

Reorientation of the lamellae occurs under large-amplitude shear flow, i.e., in the nonlinear regime of their viscoelastic response.[3] Recently, Fourier transform (FT) rheology has been introduced as a tool to quantify the nonlinear response to large-amplitude oscillatory shear (LAOS) by analysis of higher harmonics in the torque response.[24] It is, therefore, natural to apply this approach to the study of lamellar alignment of block copolymers[25] to determine the degree of nonlinear response. For ex-situ characterization, samples were taken at specific points and analyzed by 2D X-ray scattering.[26−28] Once the relation between nonlinear response under LAOS and alignment is established, the alignment kinetics might then be followed directly by FT rheology without a complex in-situ device.

The application of LAOS conditions on lamellar diblock copolymers is a well-established method to obtain macroscopic alignment of the microphase-separated structure[29−37] with three different orientation directions of the oriented lamellae (see Figure 1). The preferred orientation in the course of the orientation process depends strongly on the experimental parameters.[19] For LAOS experiments with parallel plate geometries it has been shown[20,18] that the four most important parameters are frequency (ω_1), strain amplitude (γ_0), temperature (T), and the duration of shear. For temperatures close to the order−disorder transition temperature (T_{ODT})[39,40] and for long shear times (approximately 10 h), the preferred orientations detected are either parallel or perpendicular. For a polystyrene−polyisoprene block copolymer (PS-*b*-PI) under these experimental conditions an orientation diagram was recently constructed,[38] suggesting that the state of orientation depends on an effective shear rate as in similar experiments on lyotropic lamellar phases.[41,42]

Figure 2 shows such an orientation diagram for a lamellar PS-*b*-PI (50% volume fraction for each block, overall molecular weight of 20 000 g/mol, $T_{ODT} - T_{exp} = 15$ K). The solid arrows indicate the parameters used for the experiments (see below). Because of the fact that a parallel plate geometry was used for the orientation/reorientation experiments, the shear amplitude γ_0

[†] polyMaterials AG.
[‡] Max-Planck-Institut für Polymerforschung.
[§] Cornell University.
* To whom correspondence should be addressed.

10.1021/ma0115693 CCC: $22.00 © 2002 American Chemical Society
Published on Web 03/09/2002

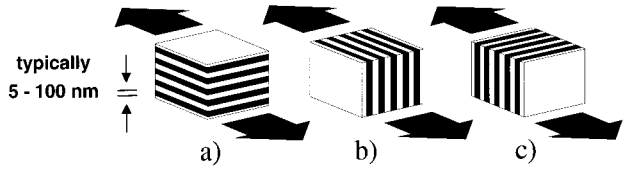

Figure 1. Possible schematic orientations of a lamellar diblock copolymer under LAOS conditions: (a) parallel, (b) perpendicular, and (c) transversal.

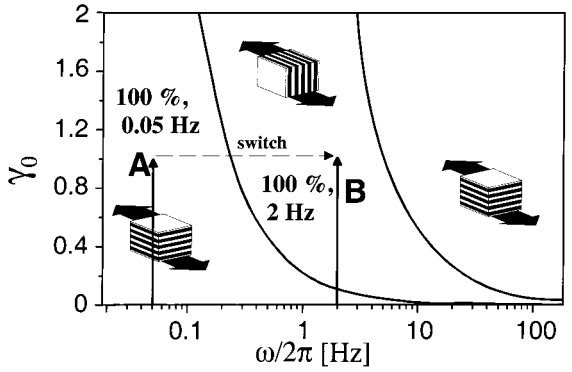

Figure 2. Schematic orientation diagram of the stable macroscopic orientation of a lamellar PS-*b*-PI under LAOS conditions. The solid arrows show the experimental conditions used for this study.

applied to the sample is a spatialy inhomogeneous and linear function of the sample radius. It increases from the center ($\gamma_0 = 0$) to the edge ($\gamma_0 = 1$) of the sample. Two shear frequencies, $\omega/2\pi = 0.05$ Hz and $\omega/2\pi = 2$ Hz, were applied.

Theoretical Background

The mathematical concepts of FT rheology are well documented[25,43−49,52] and will not be repeated here. In short, oscillatory shear with a frequency ω_1 and a strain amplitude γ_0 in the nonlinear regime results in the formation of mechanical odd higher harmonics at $3\omega_1$, $5\omega_1$, $7\omega_1$, and so forth for the torque response. The amplitudes and phases of the higher harmonics within the torque signal can be detected as spectra $I(\omega)$ in Fourier space. In this article the development of the intensity of the third harmonic relative to the fundamental $I(3\omega_1)/I(\omega_1)$ will be used to quantify the nonlinear response. For convenience we define $I(3\omega_1)/I(\omega_1) \equiv I_3/I_1$.

For quantitative interpretation of the 2D SAXS data, the order parameters $\langle \bar{P}_2 \rangle$ of the different samples were calculated from the X-ray patterns. The equations for these data processing are well documented in the literature.[50] The degree of order for a sample is given by the azimuthal width of the scattering reflex. The order parameter for a lamellar sample can be mathematically described by a three-dimensional probability distribution of the normal vector of the microscopic lamellae.[51] The scattering pattern is a projection of the probability distribution onto the plane perpendicular to the direction of the X-ray beam (detection area).

Experimental Section

The PS-*b*-PI diblock copolymer was synthesized via anionic polymerization.[4,52−54] For initiation, *sec*-butyllithium was added quickly to a solution of styrene in cyclohexane to get a narrow molecular weight distribution. After 6 h of polymerization time polyisoprene was added to the living chain ends to form the block copolymer. A few milliliters of degassed methanol was used to terminate the polymerization reaction after an additional 6 h. The monomers and the solvent were purified before use in a glovebox. Afterward, 2,6-di-*tert*-butyl-4-methylphenol (weight fraction of 0.1%) was added as an antioxidant, and the polymer was precipitated in methanol. The molecular weights of the two blocks are 10 700 g/mol for PS and 9200 g/mol for PI, determined by GPC of the precursor and liquid-state ^{1}H NMR of the final copolymer, which leads to a volume fraction of 50% for each block. All samples used for this publication originated from the same batch of the synthesis. The glass transition temperatures of 347 K for the PS block and 210 K for the PI block were determined by DSC at a heating rate of 20 K/min. The order−disorder transition temperature (T_{ODT}) was 433 K, detected by a significant decrease of the temperature-dependent storage modulus $G'(T)$, using a frequency of $\omega/2\pi = 0.05$ Hz, a strain amplitude of $\gamma_0 = 0.03$, and a heating rate of 0.3 K/min. For both dynamic-mechanical and orientation plus reorientation experiments, a Rheometrics ARES rheometer was used. The relative intensity of the third harmonic (I_3/I_1) was determined by the rheometer and displayed as "nonlinear monitoring". Additionally, the raw time data of the resulting torque were externally collected and digitized by National Instruments LabView software during the experiments.[49] In portions of 25 oscillations the collected data were processed and Fourier transformed using a home-written routine for the PV-Wave software to verify the calculation of the rheometer. In this article the nonlinear monitoring as displayed by the ARES instrument was used to follow the nonlinear behavior of the sample. All samples were annealed at T_g (PS) + 20 K for more than 24 h before the LAOS experiments were performed, which was found to be very important to gain reproducibility of the microstructural orientation.[55]

The orientation of the lamellae in the parallel direction was obtained using the following conditions as illustrated in Figure 2 (see arrow A): 50 mm parallel plate geometry, gap = 1 mm, $\omega_1/2\pi = 0.05$ Hz, $\gamma_0 = 1$, $T = 418$ K, $t = 10$ h. Immediately afterward the following conditions were applied to macroscopically reorient the lamellae from the parallel to the perpendicular orientation: $\omega_1/2\pi = 2$ Hz, $\gamma_0 = 1$, $T = 418$ K, $t = 10$ h (arrow B in Figure 2).

The use of the parallel plate geometry causes a gradient of the strain amplitude along the radial vector. The solid arrows in Figure 2 display the strain gradient from $\gamma_0 = 0$ to $\gamma_0 = 1$ applied from the inside to the outside of the sample. A sudden increase in shear frequency might macroscopically reorient the lamellae and can graphically be depicted by a horizontal shift along a fixed strain amplitude from the left of the diagram (A) along the dotted arrow to the right (B).

During the entire experiments G' and G'' were monitored. Both moduli and visual inspection did not give any indication of edge fracture of the samples under investigation. To determine the orientation of the lamellar microphase separation at different local strain values, the samples were rapidly cooled to room temperature within about 10 min, whereby the state of orientation is frozen into the glass of the PS blocks. Then the samples were cut into six tangential stripes (1 mm × 1 mm × 5 mm) and one radial stripe (1 mm × 1 mm × 25 mm) as described in the literature,[29] and the stripes were investigated by 2-dimensional small-angle X-ray scattering (2D SAXS) measurements to get X-ray patterns for all three Cartesian directions. The patterns in Figure 3 and Figure 5 were taken from the radial stripes and from the tangential stripes at $\gamma_0 = 0.5$ between the center and the edge of the sheared sample whereas the amount of parallel and perpendicular orientation for eqs 1 and 2 was calculated from the X-ray pattern along the radial stripes. For the 2D SAXS experiments a Rigaku Rotaflex X-ray source with a wavelength of 0.154 nm (Cu Kα) was employed. A three-pinhole collimator was used to generate a beam with a diameter of 0.1 mm. Scattering patterns were recorded on a 2-dimensional Siemens X-1000 area detector with a sample-to-detector distance of 137 cm. The q-vector can be detected in the range 0.15−1.5 nm^{-1}.

As illustrated in Figure 3, parallel alignment manifests itself by the presence of reflexes in the radial and tangential direction, whereas a perpendicular orientation results in

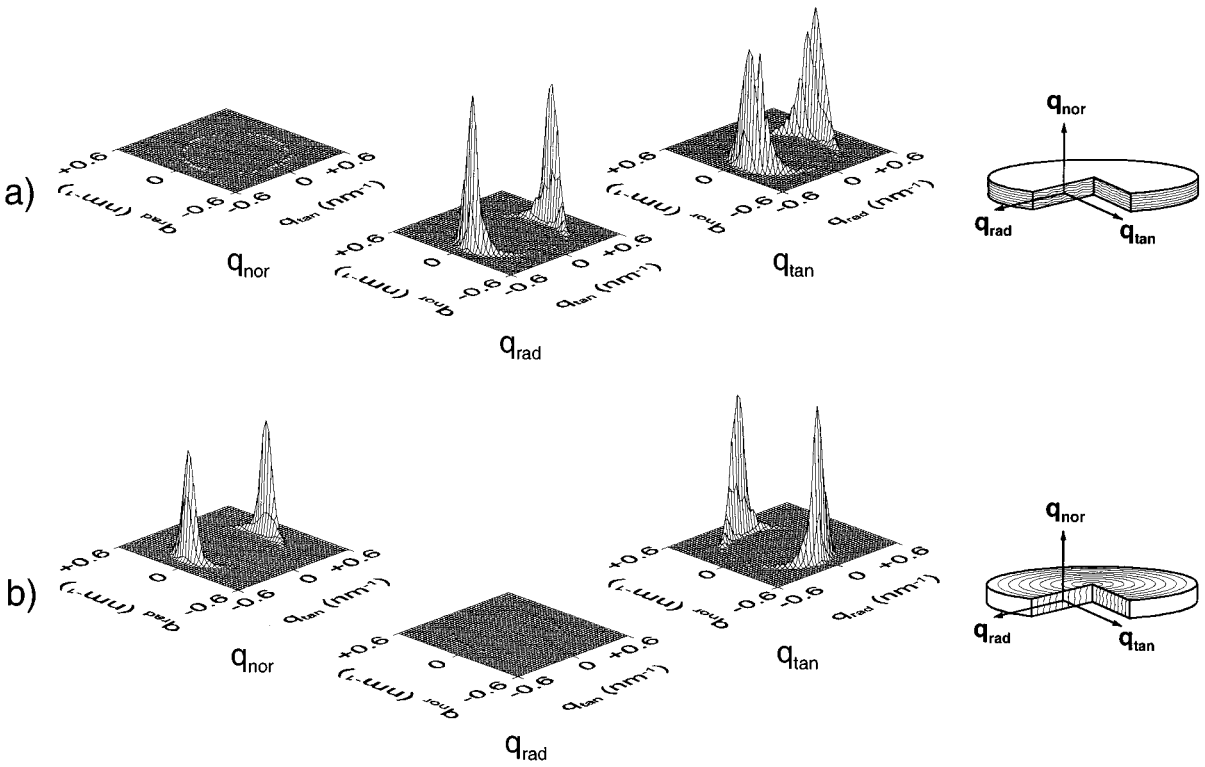

Figure 3. 2D SAXS patterns of a radial and tangential stripe of PS-*b*-PI samples at $\gamma_0 = 0.5$ in three Cartesian directions (normal, radial, and tangential) after (a) 10 h of prealignment and after (b) 20 h of total experimental time to investigate the presence of (a) parallel and (b) perpendicular orientation of the lamellae.

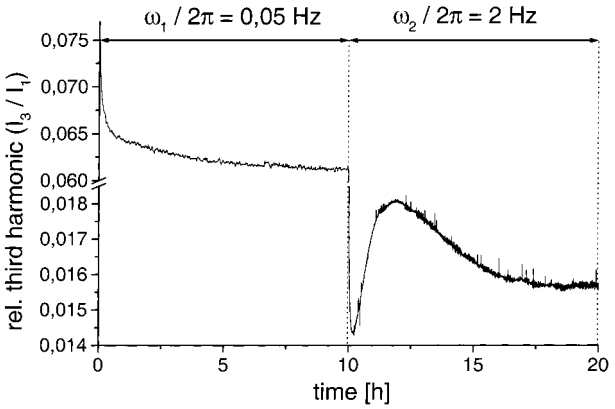

Figure 4. Relative intensity of the third harmonic I_3/I_1 during the 20 h macroscopic orientation/reorientation process.

reflexes in the normal and tangential direction. The patterns in the tangential direction are basically rotated by 90° if the sample moves from parallel to perpendicular alignment (for comparison, see Figure 3a,b).

Results

Two-Step Experiment Analyzed after a Long Time. A first LAOS experiment was performed with the conditions that result in a macroscopic parallel orientation ($\omega_1/2\pi = 0.05$ Hz, $\gamma_0 = 1$, $T = 418$ K). During the orientation process the development of the third harmonic was followed via Fourier transform rheology. After 10 h of shear the small-angle X-ray patterns are consistent with the expected parallel alignment of the lamellar microstructure (Figure 3a). The reflexes in the radial and the tangential direction clearly indicate the presence of a macroscopic parallel orientation. The order parameter of the lamellar alignment of this sample was determined to $\langle \bar{P}_2 \rangle = 0.51$.

A second sample was oriented for 10 h under the same conditions. Afterward, the parameters for the orientation process were changed to those indicated by arrow B in Figure 2 ($\omega_1/2\pi = 2$ Hz, $\gamma_0 = 1$, $T = 418$ K). These conditions were maintained for 10 h in order to get an overall perpendicular orientation. During this extended time, the macroscopic reorientation process of the lamellae from parallel to perpendicular is expected. The relative intensity of the third harmonic was measured by FT rheology to follow the nonlinear behavior of the polymer for this process. The SAXS patterns obtained from this sample in the three Cartesian directions after a total experimental shear time of 20 h are shown in Figure 3b. Reflexes in the normal and the tangential direction are consistent with the expected perpendicular orientation of the lamellae. The order parameter for the perpendicular alignment of the sample was calculated to $\langle \bar{P}_2 \rangle = 0.75$. The application of the higher frequency resulted in a higher degree of orientation as compared to the parallel orientation achieved in the lower frequency regime.

The development for the relative intensity of the third harmonic during such an experiment with 10 h of macroscopic parallel prealignment and 10 h of macroscopic reorientation to form the perpendicular alignment is shown in Figure 4. The relative intensity of the third harmonic decays monotonically in the first 10 h in a quasi-stretched exponential fashion from $I_3/I_1 = 0.077$ to an asymptotic plateau value of $I_3/I_1 = 0.061$ during the generation of the parallel orientation. Afterward, the conditions were changed to force the lamellae into a perpendicular orientation. At the beginning of the macroscopic reorientation process the relative intensity of the third harmonic decays to an overall minimum of $I_3/I_1 = 0.014$, which is reached after 10 min. Then it increases steeply to reach a maximum value of $I_3/I_1 =$

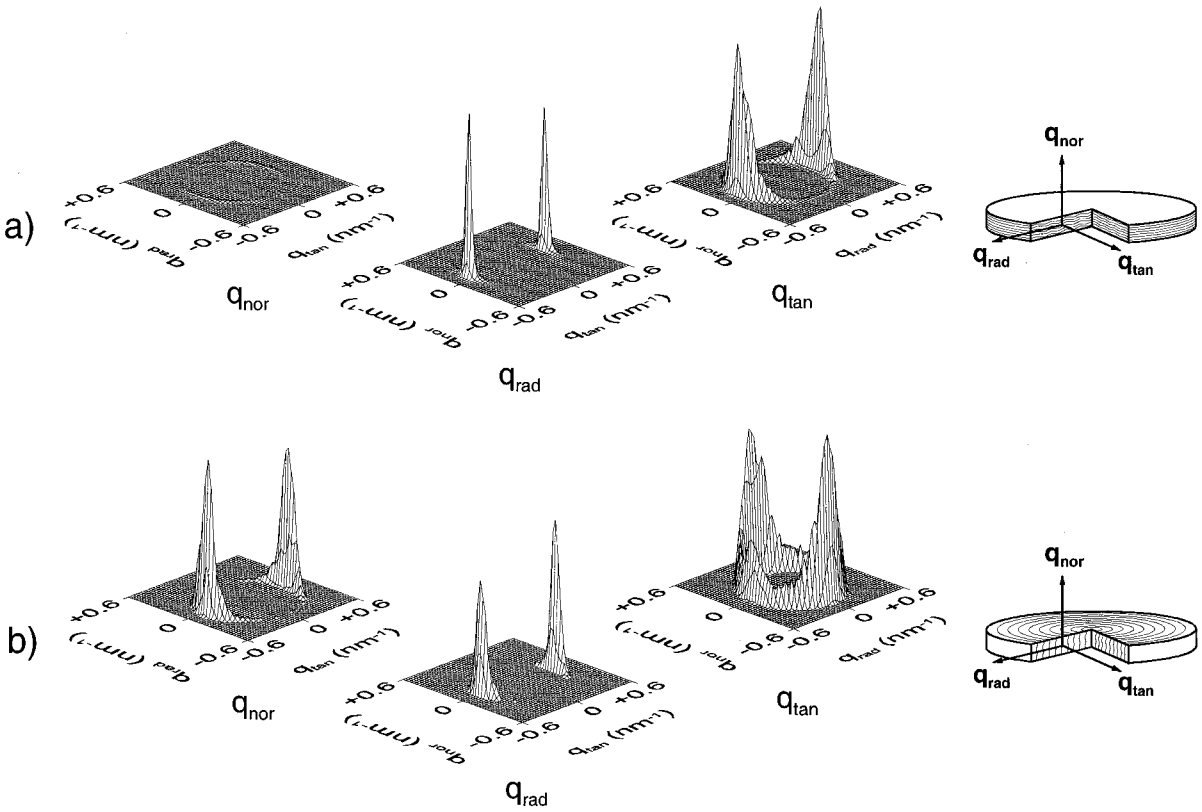

Figure 5. 2D SAXS patterns of a radial and tangential stripe of PS-*b*-PI samples at $\gamma_0 = 0.5$ in three Cartesian directions (normal, radial, and tangential) after the following conditions: (a) preorienting for 10 h at $\omega_1/2\pi = 0.05$ Hz ($\gamma_0 = 1$, see Figure 3a) and changing to $\omega_1/2\pi = 2$ Hz ($\gamma_0 = 1$) for 10 min; (b) preorienting for 10 h at $\omega_1/2\pi = 0.05$ Hz ($\gamma_0 = 1$) and changing to $\omega_1/2\pi = 2$ Hz ($\gamma_0 = 1$) for 1 h to investigate the presence of (a) parallel and (b) bimodal orientation of the lamellae.

0.018 in the next 1−2 h. The further and final decay of the third harmonic shows an asymptotic decrease to a terminal plateau value of $I_3/I_1 = 0.016$ at the end of the 20 h shear experiment. At this time there is an overall perpendicular orientation, as shown by small-angle X-ray scattering patterns in Figure 3b. Reproducibility was checked for the shape and numerical values of these measurements. The numerical values for the relative intensity of the third harmonic depend on the mechanical history of the sample before the experiment and can offset in a range of 5% while the time development was fully reproducible.

For comparison, polyisoprene and polystyrene homopolymers with the same molecular weight and the same T_g as the two blocks of the copolymer were measured at $\omega_1/2\pi = 2$ Hz and $\gamma_0 = 1$. The polystyrene sample did cause a relative intensity of the third harmonic of $I_3/I_1 = 0.002$ at the temperature of the reorientation experiment. The ratio I_3/I_1 of the polyisoprene sample was only $I_3/I_1 = 0.0002$ even at room temperature, which is 120 K lower than the temperature of the experiments described above. These low values for the third harmonic suggest that nearly the whole nonlinear behavior—observed in the reorientation experiment—is not due to either of the homopolymers but results from the reorientation of the lamellae.

Relation between Nonlinear Flow and Alignment. To better understand the relation between nonlinear flow and structural reorganization of the lamellae, several additional orientation experiments were performed with different experimental times for the macroscopic reorientation process as suggested by the time evolution of the third harmonic of Figure 4. Subsequent 2D SAXS measurements were performed to correlate nonlinear response with orientation behavior at different times.

In Figure 4 the most intriguing feature of the time development of the ratio I_3/I_1, which monitors the nonlinear response, is the pronounced drop after increase of the shear frequency. To study the underlying structural changes in more detail, a sample was first oriented for 10 h to form the parallel prealignment, and then the frequency was increased to 2 Hz (arrow B in Figure 2) for a duration of only 10 min. This time was specifically chosen to stop the experiment at the minimum intensity of the third harmonic as displayed in Figure 4. The 2D SAXS patterns of this sample are shown in Figure 5a. The comparison between these scattering reflexes and the reflexes of the sample which was only preoriented at $\omega_1/2\pi = 0.05$ Hz (Figure 3a) shows that the sample is still ordered in a parallel way. The significant difference between these two orientations is the magnitude of the order parameter, which has increased to a higher value $\langle \bar{P}_2 \rangle = 0.78$. Thus, only 10 min of higher frequency leads to a value more than 50% higher than achieved for the lower frequency conditions after 10 h.

This reveals that the application of a higher frequency after parallel prealignment does not immediately force the lamellae of the sample into the perpendicular orientation. Instead, during the first 10 min the parallel alignment remains but with its order significantly improved. We suppose that this is directly related to the decrease of the relative intensity of the third harmonic as shown in Figure 4.

The further development of the third harmonic reveals an increase during the next 2 h of applying the higher shear frequency to a maximum of $I_3/I_1 = 0.018$.

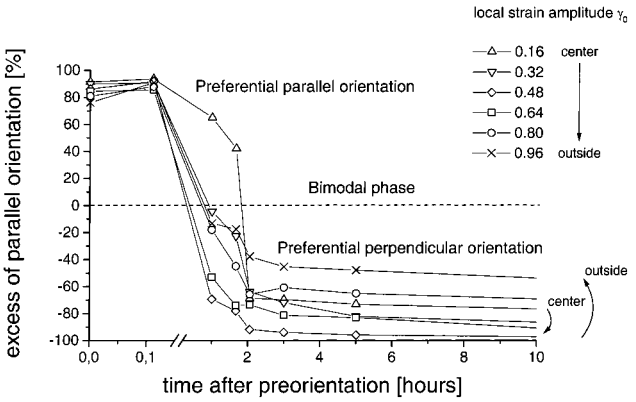

Figure 6. Time evolution of the alignment after application of the higher shear frequency. The orientation of the samples was investigated by the integration of the tangential 2D SAXS patterns. The displayed 48 data points reflect each the analysis of three 2D SAXS patterns.

To unravel the underlying orientation process, we investigated several samples with small-angle X-ray scattering which were quenched after 10 h of parallel prealignment and an additional 1−2 h of the reorientation process. The 2D SAXS patterns of a sample that was exposed to the higher shear frequency for exactly 1 h are displayed in Figure 5b.

The patterns reveal a bimodal orientation consisting of a mixture of parallel and perpendicular oriented lamellae. The reorientation time of 1 h corresponds to the maximum of the third harmonic. Thus, increase in the third harmonic seems to be related to the reorientation of the lamellae. The further development of the relative intensity of the third harmonic displays a monotonic decrease which levels off at 0.016 after 10 h of applying the higher frequency. The investigation of the final orientation by small-angle X-ray scattering (Figure 3b) reveals a perpendicular alignment on a macroscopic scale. A constant value for the third harmonic after 20 h of shear indicates the end of the reorientation process under these conditions and the presence of a dynamic steady state.

Orientation Distribution as a Function of Alignment Duration. For better interpretation and quantification of these observations the 2D-SAXS patterns, measured along the radius of the samples for particular points of the trajectory of the third harmonic, were analyzed in a second way. As discussed above, parallel and perpendicular alignment both give rise to scattering peaks in the tangential direction, yet perpendicular to each other. The ratio of these peaks varies along the sample radius as determined by analyzing six different points of the radial stripe. The results will be discussed in terms of an excess of parallel orientation (epo) defined in eq 1, varying between −1 and +1.

$$\mathrm{epo} \equiv \frac{A_{\mathrm{par}} - A_{\mathrm{perp}}}{A_{\mathrm{par}} + A_{\mathrm{perp}}}$$

where A_{par} is the area of the integrated parallel 2D SAXS reflex in the tangential direction and A_{perp} is the area of the integrated perpendicular 2D SAXS reflex in the tangential direction.

Results of this analysis are displayed in Figure 6. Different symbols correspond to different sample radii. For data interpretation one has to keep in mind that the applied strain amplitude γ_0 varies with the diameter from 0 at the center to 1 at the sample rim. An excess of parallel orientation is displayed by positive values in Figure 6 whereas an excess of perpendicular orientation results in negative values.

The macroscopic reorientation process after preorientation starts with a parallel oriented sample. In the first 10 min the excess of parallel orientation slightly increases throughout the sample as shown by the 2D SAXS patterns of Figure 5a. The time dependence of the change in the parallel alignment at longer times follows the time dependence of the third harmonic. The excess of parallel orientation rapidly decreases to reach the region where the areas of the integrated SAXS patterns of the parallel and the perpendicular alignment are comparable in magnitude. This matches the development of the third harmonic in Figure 4 which reaches a maximum after 1−2 h of reorientation conditions corresponding to a maximum bimodal microstructure. The further decrease of the excess of parallel orientation is due to the formation of a macroscopic perpendicular orientation of the microphase until the end of the 20 h experiment.

For the different sample radii the overall development of the excess of parallel orientation is basically the same, but two differences are noticeable:

(1) At the end of the preorientation procedure, the magnitude of the excess of parallel orientation increases from the outside to the inside of the sample. This is in qualitative agreement with the orientation scheme in Figure 2. Arrow A represents the orientation conditions used for the first 10 h of the experiment. The shear amplitude ranges from $\gamma_0 = 0$ to $\gamma_0 = 1$ along the radius. The arrow represents the increasing strain amplitude from the center to the edge of the sample. The higher strain values at the edge of the sample are much closer to the regime of the perpendicular alignment than the lower strain values. Therefore, it seems reasonable that the excess of parallel orientation in the center of the sheared sample is higher.

(2) At the end of the total experimental time, the lowest value for epo, which is the best perpendicular alignment, is found in the middle of the sample, between the center and the edge, at a strain value of $\gamma_0 = 0.5$. At the center and the edge of the sample the excess of parallel orientation is considerably higher. The conditions of the macroscopic reorientation procedure are shown in Figure 2 by arrow B. The onset and the end of the arrow represent the center and the edge of the sample. Both points are closer to or even within the regimes of parallel alignment. Therefore, it seems reasonable that the orientation of the microphase at these points of the sample is affected by the proximity of the parallel regimes, and the lowest excess of parallel orientation, i.e., the highest amount of perpendicular orientation, is found in the region of intermediate strain amplitudes.

Clearly, on the time scale investigated here the reorientation of the lamellae occurs in a largely inhomogeneous fashion within the sample. The nonlinear rheological response, however, is measured averaging over the entire sample. To better relate the two observables, the degree of bimodal alignment (dba) was defined as follows:

$$\mathrm{dba} \equiv 1 - \left| \frac{\bar{A}_{\mathrm{par}} - \bar{A}_{\mathrm{perp}}}{\bar{A}_{\mathrm{par}} + \bar{A}_{\mathrm{perp}}} \right|$$

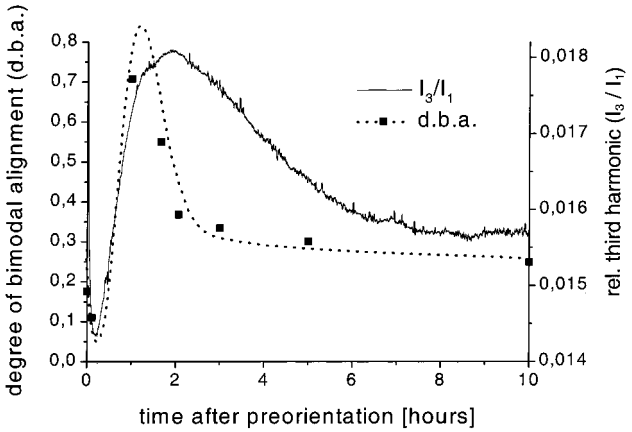

Figure 7. Comparison between the time evolution of the nonlinear mechanical response I_3/I_1 of the sample and the degree of bimodal alignment calculated by the integration of the 2D SAXS patterns in the tangential direction. The dotted line is drawn as a guide to the eyes.

The degree of bimodal alignment does not distinguish between parallel and perpendicular excess orientation and varies from 1 for a sample with equal amount of parallel and perpendicular orientation in the tangential direction to a value of 0 for a sample which only shows parallel or perpendicular alignment. In contrast to the calculation of the excess of parallel orientation, in this equation $\bar{A}_{par}$ and $\bar{A}_{perp}$ are average values of the six sample radii. The weighting factor was chosen to be proportional to the related volumes.

Results of this analysis are displayed in Figure 7 together with I_3/I_1 as a measure of the nonlinear rheological response. The relative intensity of the third harmonic follows the bimodality of the microphase orientation during the 10 h of applying a higher shear frequency $\omega_1/2\pi = 2$ Hz. In the first 10 min the third harmonic decreases like the bimodality to form improved parallel alignment with the higher order parameter. During the next 2 h both the bimodality and the third harmonic increase, and a sample whose microphase contains parallel and perpendicular oriented lamellae is formed. At the end both quantities decrease by the formation of macroscopic perpendicular alignment. It should be noted that although the two phenomena are clearly related, the two curves in Figure 7 are not identical. This points to the fact that the degree of alignment and the respective nonlinear response of the sample are not correlated in a simple manner.

Comparison with Linear Rheological Response. The mechanical behavior of our samples during the entire reorientation process by conventional rheology was also monitored. This allows to investigate whether the measurement of the storage modulus G' or the loss modulus G'' can give similar information as the relative intensity of the third harmonic during the orientation/reorientation process. For this purpose these quantities are displayed in Figure 8. As does the third harmonic, both the storage modulus G' and the loss modulus G'' decay in the first 10 h during the prealignment of the microphase. After changing to the reorientation conditions, the moduli increase drastically due to the higher shear frequency. In the first 10 min of the macroscopic reorientation process, G' and G'' decrease subsequently to a relative minimum correlated with the formation of a parallel orientation with a much higher order parameter.

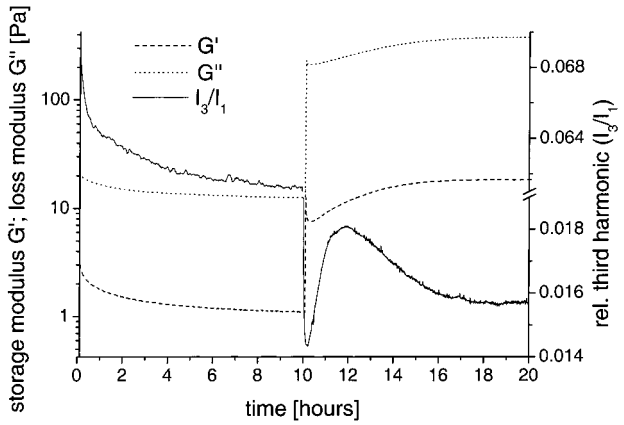

Figure 8. Development of the storage modulus G', the loss modulus G'', and the relative intensity of the third harmonic I_3/I_1 as a function of time during the orientation and reorientation process.

The onset of the macroscopic reorientation of the lamellae leads to an increase of G' and G'' similar to the increase of the relative intensity of the third harmonic, and both moduli approach asymptotically the final plateau values. This ensures the validity of our experiments. Comparing linear and nonlinear response, the most evident difference between these quantities is that, in contrast to G' and G'', the third harmonic goes through a maximum corresponding to the formation of a bimodal orientation distribution after approximately 2 h of the reorientation process.

In summary, the high values of G' and G'' confirm that in the perpendicular alignment the linear response is dominated by polystyrene. In contrast, the relative intensity of the third harmonic follows the development of the bimodality in Figure 7 much better. Thus, the nonlinear response provides adding external information a more efficient monitor of the complex reorientation process.

Conclusions

The results presented clearly show that the reorientation of the lamellae under LAOS conditions in parallel plate geometry occurs in a spatially inhomogeneous fashion. To follow this complex process, ideally knowledge of the entire orientation distribution function is needed as a function of time. This is achieved by 2D SAXS and allows the detection of bimodal orientation distributions, which are difficult to identify if only moments (order parameters) of the distribution are measured.

Monitoring the linear rheological behavior, such as the storage modulus G', is not sufficient, because its behavior in time can be explained as follows: Under the applied experimental conditions the polystyrene is 71 K above its glass transition point whereas the isoprene phase is about 208 K above its T_g. Thus, the storage modulus G' of the overall sample decreases by the formation of the parallel alignment because the polystyrene layers can slide easily in between the liquidlike polyisoprene layers for a fixed strain amplitude and increases as the perpendicular alignment is formed, where the polystyrene itself has to be sheared. G' indicates the improvement in the parallel alignment during the first 10 min after increasing the shear frequency but fails to differentiate between a bimodal and a uniform perpendicular alignment. Contrary to

that, under the experimental conditions applied here, the relative degree of nonlinear response is low for both parallel and perpendicular alignment, where one of the two blocks dominates the storage modulus.

Thus, the nonlinear response provides additional information as it monitors misalignments, and it can detect both the improvement of the alignment as a function of time and the presence of a bimodal distribution. Since the detection of mechanical higher harmonics has become highly sensitive,[47,49,56,57] the complex alignment process can easily be followed online in the future.

In the present study we have demonstrated that the nonlinear mechanical response of a lamellar sample under shear is sensitive to the development of bimodal orientation distributions. These measurements can be performed using the same equipment used to generate the large-amplitude oscillatory shear. Only if the orientation behavior of the investigated block copolymer system under the applied conditions is well-known, e.g., from scattering or microscopy, the development of the orientation processes within a series of similar systems can be followed more easily by FT rheology. Thus, these measurements are a useful and complementary tool to the existing common techniques.

Acknowledgment. The authors thank Dr. H. Leuninger and Dr. P. Reinheimer for their initial work on "orientation of block copolymers" and "Fourier transform rheology" and subsequent assistance. We also thank Dr. D. van Dusschoten for discussions and technical improvements toward the FT-Rheology technique. Financial support from the BASF AG and the EU-project CAPS (Complex Architecture in Diblock Copolymer Based Polymer Systems), nr. FMRX-CT97-0112 (DG 12-DLCL) is gratefully acknowledged. U.W. thanks for support by the National Science Foundation DMR-0072009 and the Cornell Center for Materials Research (NSF DMR-9632275). Finally, thanks to D. Babski and M. Pollard for carefully checking the manuscript.

References and Notes

(1) Macosko, C. W. *Rheology: Principles, Measurement, and Applications*; VCH: New York, 1994.
(2) Malkin, A. Y. *Rheol. Acta* **1995**, *34*, 27.
(3) Zhang, Y.; Wiesner, U.; Spiess, H. W. *Macromolecules* **1995**, *28*, 778.
(4) Tepe, T.; Schulz, M. F.; Zhao, J.; Tirrell, M.; Bates, F. S.; Mortensen, K.; Almdal, K. *Macromolecules* **1995**, *28*, 3008.
(5) Gupta, V. K.; Krishnamoorti, R.; Kornfield, J. A.; Smith, S. D. *Macromolecules* **1995**, *28*, 4464.
(6) Bodycomb, J.; Hashimoto, T. *Int. J. Thermophys.* **1999**, *20*, 857.
(7) Leibler, L. *Macromolecules* **1980**, *13*, 1602.
(8) Bates, F. S.; Fredrickson, G. H. *Annu. Rev. Phys. Chem.* **1990**, *41*, 525.
(9) Fredrickson, G. H.; Bates, F. S. *Ann. Rev. Mater. Sci.* **1996**, *26*, 501.
(10) Matsen, M. W.; Bates, F. S. *Macromolecules* **1996**, *29*, 1091.
(11) Semenov, A. N. *Sov. Phys. JETP* **1982**, *61*, 733.
(12) Neumann, C.; Loveday, D. R.; Abetz, V.; Stadler, R. *Macromolecules* **1998**, *31*, 2493.
(13) Hamley, I. W. *The Physics of Block Copolymers*; Oxford University Press: Oxford, 1998.
(14) Han, C. D.; Baek, D. M.; Kim, J. K.; Ogawa, T.; Sakamoto, N.; Hashimoto, T. *Polymer* **1998**, *39*, 4679.
(15) Fischer, H.; Weidisch, R.; Stamm, M.; Budde, H.; Horing, S. *Colloid Polym. Sci.* **2000**, *278*, 1019.
(16) Daniel, C.; Hamley, I. W.; Mingvanish, W.; Booth, C. *Macromolecules* **2000**, *33*, 2163.
(17) Maier, G.; Fenchl, A.; Sigl, G. *Macromol. Chem. Phys.* **1997**, *198*, 137.
(18) Gupta, V. K.; Krishnamoorti, R.; Chen, Z. R.; Kornfield, J. A.; Smith, S. D.; Satkowski, M. M.; Grothaus, J. T. *Macromolecules* **1996**, *29*, 875.
(19) Chen, Z. R.; Issaian, A. M.; Kornfield, J. A.; Smith, S. D.; Grothaus, J. T.; Satkowski, M. M. *Macromolecules* **1997**, *30*, 7096.
(20) Polis, D. L.; Smith, S. D.; Terrill, N. J.; Ryan, A. J.; Morse, D. C.; Winey, K. I. *Macromolecules* **1999**, *32*, 4668.
(21) Pople, J. A.; Hamley, I. W.; Fairclough, J. P. A.; Ryan, A. J.; Hill, G.; Price, C. *Polymer* **1999**, *40*, 5709.
(22) Makinen, R.; Ruokolainen, J.; Ikkala, O.; de Moel, K.; ten Brinke, G.; De Odorico, W.; Stamm, M. *Macromolecules* **2000**, *33*, 3441.
(23) Hamley, I. W.; Pople, J. A.; Fairclough, J. P. A.; Terrill, N. J.; Ryan, A. J.; Booth, C.; Yu, G. E.; Diat, O.; Almdal, K.; Mortensen, K.; Vigild, M. *J. Chem. Phys.* **1998**, *108*, 6929.
(24) Wilhelm, M.; Maring, D.; Spiess, H. W. *Rheol. Acta* **1998**, *37*, 399.
(25) Daniel, C.; Hamley,I. W.; Wilhelm, M.; Mingvanish, W. *Rheol. Acta* **2001**, *40*, 39.
(26) Alexander, L. E. *X-ray Diffraction Methods in Polymer Science*; Krieger Publishing Co.: Huntington, 1979.
(27) Glatter, O.; Kratky, O. *Small-Angle X-ray Scattering*; Academic Press: London, 1982.
(28) Feigin, L. A.; Svergun, D. I. *Structure Analysis by Small-Angle X-ray Scattering;* Plenum Press: New York, 1987.
(29) Hadziioannou, G.; Mathis, A.; Skoulios, A. *Colloid Polym. Sci.* **1979**, *257*, 136.
(30) Hadziioannou, G.; Picot, C.; Skoulios, A.; Ionescu, M. L.; Mathis, S.; Duplessix, R.; Gallot, Y.; Lingelser, J. P. *Macromolecules* **1982**, *15*, 263.
(31) Lodge, T. P.; Fredrickson, G. H. *Macromolecules* **1992**, *25*, 5643.
(32) Wiesner, U. *Macromol. Chem. Phys.* **1997**, *198*, 3319.
(33) Chen, Z. R.; Kornfield, J. A. *Polymer* **1998**, *39*, 4679.
(34) Hajduk, D. A.; Tepe, T.; Takenouchi, H.; Tirrell, M.; Bates, F. S.; Almdal, K.; Mortensen, K. *J. Chem. Phys.* **1998**, *108*, 326.
(35) Pinheiro, B. S.; Winey, K. I. *Macromolecules* **1998**, *31*, 4447.
(36) Laurer, J. H.; Pinheiro, B. S.; Polis, D. L.; Winey, K. I. *Macromolecules* **1999**, *32*, 4999.
(37) Vigild, M. E.; Chu, C.; Sugiyama, M.; Chaffin, K. A.; Bates, F. S. *Macromolecules* **2001**, *34*, 951.
(38) Leist, H.; Maring, D.; Thurn-Albrecht, T.; Wiesner, U. *J. Chem. Phys.* **1999**, *110*, 8225.
(39) Rosedale, J.; Bates, F. S.; Almdal, K.; Mortensen, K.; Wignall, G. D. *Macromolecules* **1995**, *28*, 1429.
(40) Tepe, T.; Hajduk, D. A.; Hillmyer, M. A.; Weimann, P. A.; Tirrell, M.; Bates, F. S.; Almdal, K.; Mortensen, K. *J. Rheol.* **1997**, *41*, 1147.
(41) Berghausen, J.; Zipfel, J.; Lindner, P.; Richtering, W. *Europhys. Lett.* **1998**, *43*, 683.
(42) Berghausen, J.; Zipfel, J.; Diat, O.; Narayanan, T.; Richtering, W. *Phys. Chem. Chem. Phys.* **2000**, *2*, 3623.
(43) Krieger, I. M.; Tyan-Faung, N. *Rheol. Acta* **1973**, *12*, 567.
(44) Giacomin, A. J.; Dealy, J. M. *Techniques in Rheological Measurements*; Chapman and Hall: London, 1993; Chapter 4, p 99.
(45) Ramirez, R. W. *The FFT Fundamentals and Concepts*; Prentice-Hall: Engelwood Cliffs, NJ, 1995.
(46) Reimers, M. J.; Dealy, J. M. *J. Rheol.* **1996**, *40*, 167.
(47) Wilhelm, M.; Reinheimer, P.; Ortseifer, M. *Rheol. Acta* **1999**, *38*, 349.
(48) Reinheimer, P.; Wilhelm, M.; Langela, M.; Leuninger, H.; Wiesner, U.; van Dusschoten, D. *XIIIth International Congress On Rheology*; Cambridge, UK, 2000; pp 1−287.
(49) Wilhelm, M.; Reinheimer, P.; Ortseifer, M.; Neidhöfer, T.; Spiess, H. W. *Rheol. Acta* **2000**, *39*, 241.
(50) Ehrlich, D.; Takenaka, M.; Okamoto, S.; Hashimoto, T. *Macromolecules* **1993**, *26*, 189.
(51) Windel, A. H.; Ward, I. M. *Developments in Oriented Polymers*, 1st ed.; Applied Science Publishers: London, 1982.
(52) Flory, P. J. *Principles of Polymer Chemistry*; Cornell University Press: Ithaca, NY, 1979.
(53) Elias, H. G. *An Introduction to Polymer Science*; VCH: New York, 1997.
(54) Zhang, Y. M.; Wiesner, U. *Macromol. Chem. Phys.* **1998**, *199*, 1771.
(55) Zhang, Y.; Wiesner, U.; Yang, Y.; Pakula, T.; Spiess, H. W. *Macromolecules* **1996**, *29*, 5427.
(56) van Dusschoten, D.; Wilhelm, M. *Rheol. Acta* **2001**, *40*, 395.
(57) Wilhelm, M. *Macromol. Mater. Eng.* **2002**, *287*, 83.

MA0115693